A MIXED FINITE ELEMENT METHOD FOR CONSTRAINING AND REGULARIZING THE OPTICAL FLOW CONSTRAINT

R.B. LEHOUCQ* AND D.Z. TURNER*

24 August 2016

Abstract. The contribution of our paper is to present a mixed finite element method for estimation of the velocity in the optical flow constraint, i.e., an advection equation. The resulting inverse problem is well-known to be undetermined because the velocity vector cannot be recovered from the scalar field advected unless further restrictions on the flow, or motion are imposed. If we suppose, for example, that the velocity is solenoidal, a well-defined least squares problem with a minimizing velocity results. Equivalently, we have imposed the constraint that the underlying motion is isochoric. Unfortunately, the resulting least squares system is ill-posed and so regularization via a mixed formulation of the Poisson equation is proposed. Standard results for the Poisson equation demonstrate that the regularized least squares problem is well-posed and has a stable finite element approximation. A numerical example demonstrating the procedure supports the analyses. The example also introduces a closed form solution for the unregularized, constrained least squares problem so that the approximation can be quantified.

Key words. Optical flow, digital image correlation, transport equation, regularization, mixed finite element method

AMS subject classifications. 35F16, 65M30, 65M32, 65N20, 65N21, 65N30

1. Introduction.

Our paper describes a constrained, regularized least squares approach for estimating the velocity vector field $\mathbf{v}$ given the scalar image intensity $\phi = \phi(x, y, t)$ for a model given by the advection equation

$$\begin{cases} \phi_t + \mathbf{v} \cdot \nabla \phi = 0 & \text{over } \Omega \times (0, T)\,, \\ \phi(x, y, 0) = \phi_0(x, y) & x, y \in \Omega\,, \end{cases} \tag{1}$$

including suitable boundary conditions. Such a model represents the so-called optical flow constraint for idealized image motion given the assumption that the image intensity of an object is time independent and that spatial, temporal sampling is sufficiently resolved; see e.g., [13]

A least squares method results when we consider the formal minimization problem: Given intensity data $\hat{\phi}$, find

$$\mathbf{b}^* = \arg\min_{\mathbf{b}} \frac{1}{2} \int_0^T \int_\Omega \left(\hat{\phi}_t + \mathbf{b} \cdot \nabla \hat{\phi}\right)^2 dx\, dt\,, \tag{2a}$$

over a class of suitable functions. Proceeding formally and assuming appropriate boundary conditions, the corresponding normal equations are given by the singular linear system

$$\begin{cases} \left(\nabla \hat{\phi} \otimes \nabla \hat{\phi}\right) \mathbf{b}^* = -\hat{\phi}_t \, \nabla \hat{\phi} & \text{over } \Omega \times (0, T)\,, \\ \hat{\phi}(x, y, 0) = \phi_0(x, y) & x, y \in \Omega\,. \end{cases} \tag{2b}$$

*Center for Computing Research, Sandia National Laboratories, P.O. Box 5800, MS 1320, Albuquerque NM 87185-1320, {rblehou,dzturne}@sandia.gov. This work was supported by the Laboratory Directed Research and Development program at Sandia National Laboratories. Sandia is a multi-program laboratory operated by Sandia Corporation, a Lockheed Martin Company, for the United States Department of Energy under contract DE-AC04-94-AL85000.

Because the coefficient matrix is singular, the least squares problem (2a) is undetermined since adding

$$\bar{\mathbf{b}} := \psi J \, \nabla\hat{\phi} \,, \quad \psi\colon \Omega \to \mathbb{R} \,, \quad J := \begin{bmatrix} 0 & -1 \\ 1 & 0 \end{bmatrix} , \tag{2c}$$

to $\mathbf{b}^*$ is also a minimizer (and also a solution to the normal equations) because $\bar{\mathbf{b}} \cdot \nabla\hat{\phi} = 0$. This indeterminacy is intrinsic and explains that the velocity field cannot, in general, be reconstructed given the intensity and embodies the challenge in attempting to reconstruct a vector parameter from scalar intensity data. An important consequence is that the minimization problem (2a) is not well-defined so that the ensuing normal equations (2b) have an infinite number of solutions. We also remark that because $\phi_t = -\mathbf{v} \cdot \nabla\phi_0$ for the advection equation system (1), only the velocity in the direction of $\nabla\phi$ can ultimately be recovered—this is known as the aperture problem.

A linear constraint, however, can be imposed on the velocity so that the resulting normal equations determine a unique velocity from the space of functions defined by $\bar{\mathbf{b}}$ and $\nabla\hat{\phi}$. For instance, we can augment the equations (2b) with the constraint $\nabla \cdot \mathbf{b}^* = 0$. Equivalently, we have imposed the constraint that the underlying optical flow, or motion is isochoric. Moreover, if the true velocity is indeed solenoidal, then the velocity can be completely reconstructed. We remark, though, that our choice of a solenoidal constraint is illustrative; other constraints are possible. Ultimately, the choice of constraint depends upon the specific problem at hand and whether the choice (along with regularization) leads to a well-posed estimation problem.

The primary contribution of this work is to present a mixed finite element method for the constrained, regularized estimation of the velocity in the optical flow constraint. We show that this method resolves the aperture problem and leads to a well-posed problem, both for the infinite and finite dimensional formulations.

The first step is to constrain the minimization problem (2a) by considering: Given intensity data $\hat{\phi}$, solve

$$\underset{\mathbf{b}\in\mathcal{B}}{\arg\min}\, \frac{1}{2} \int_0^T \int_\Omega \left(\hat{\phi}_t + \mathbf{b} \cdot \nabla\hat{\phi} \right)^2 dx\, dt \,. \tag{3}$$

Our choice of constraint space is given by

$$\mathcal{B} := \{ \mathbf{b} \in H_{\mathrm{div},\Gamma}(\Omega) \,|\, \nabla \cdot \mathbf{b} = 0 \text{ over } \Omega \,, \mathbf{b} \cdot \mathbf{n} = 0 \text{ over } \Gamma \subset \partial\Omega \} \,, \tag{4}$$

where $H_{\mathrm{div},\Gamma}(\Omega) \subset H_{\mathrm{div}}(\Omega)$ is the space of vector functions that are square integrable with zero normal component along Γ and whose divergence is square integrable. However, as we show at the end of §2, the resulting optimality system is ill-posed. See [2] for an informative review on ill-posed problems in computer vision.

The second step is to regularize the least squares functional with $\nu^2/2 \int_\Omega \mathbf{b} \cdot \mathbf{b} \, dx$ resulting in a well-posed least squares problem. Equivalently, we show that our choice of regularization leads to a saddle point system containing a mixed formulation of the Poisson equation. Standard results for the Poisson equation demonstrate that the regularized system is well-posed and has a stable mixed finite element approximation. A numerical example demonstrating the procedure is presented in §4 supporting the analysis. The example also introduces a closed form solution for the unregularized, constrained least squares problem so that the approximation can be quantified. In particular, our regularized functional is an instance of an augmented Lagrange method due to Fortin and Glowinski [6]. Again, we emphasize that our choice of constraint space is motivated by physical considerations and mathematical convenience, i.e., the constraint space $\mathcal{B}$ may be replaced by another, suitable, space.

Our approach has application to digital image correlation (DIC) [12] and as the initialization step for the regularized, nonlinear least squares approach introduced in the paper [8] by Ito and Kunisch for estimating the convection coefficient that we considered in the report [9]. The DIC application is that of sequence analysis; the interested reader is referred to the discussion and overview by Aubert and Kornprobst in their textbook [1, pp. 249–256].

1.1. Related Approaches. The conventional approach within the DIC community to regularize the indeterminacy of the normal equations (2b) is to introduce a collection of points in a neighborhood about $\mathbf{x}$; the collection defines a subset; see, e.g., [12, pp.85–86]. Such an approach is tantamount to regularizing the corresponding discrete, ill-posed problem by removing the singularity for the coefficient matrix. Unfortunately, such a discrete problem is ill-conditioned since the indeterminacy has not been incorporated into the problem. The manifestation of this pitfall is the basis for the well-known sensitivity upon the size of a subset in DIC.

The landmark paper [7] by Horn and Schunck formally introduced a regularized approach for estimating the velocity; a precise variational formulation of the infinite dimensional problem was given by Schnörr in [11] who demonstrated that the regularized least squares problem was well-posed over $[H^1(\Omega)]^2$. However, the Horn and Schunck approach never confronted the indeterminacy associated with estimating the velocity. An important consequence of our analysis is that a constraint must be incorporated into the least squares problem in order to confront the indeterminacy.

2. A Saddle Point Problem. We augment the constrained minimization problem (3) by including a regularization term. This term converts the ill-posed problem (3), which we establish at the end of this section, into a well-posed problem. This results in the following regularized, minimization problem: Given intensity data $\phi \in H^1_{\partial\Omega/\Gamma}(\Omega) \times (0,T)$, solve

$$\mathbf{b}^\nu = \underset{\mathbf{w}\in\mathcal{B}\times(0,T)}{\arg\min}\, \frac{1}{2}\int_0^T \left\{ \int_\Omega \left(\phi_t + \mathbf{w}\cdot\nabla\phi\right)^2 dx + \nu^2 \int_\Omega \mathbf{w}\cdot\mathbf{w}\, dx \right\} dt\,, \tag{5}$$

where the space $\mathcal{B}$ was defined in (4) and $H^1_{\partial\Omega/\Gamma}(\Omega)$ is the space of functions in $H^1(\Omega)$ that are zero on $\partial\Omega/\Gamma$. In order to solve this minimization problem, we introduce the Lagrange functional

$$F(\mathbf{w},\lambda^\nu) = \frac{1}{2}\int_0^T \left\{ \int_\Omega \left(\phi_t + \mathbf{w}\cdot\nabla\phi\right)^2 dx + \nu^2 \int_\Omega \mathbf{w}\cdot\mathbf{w}\, dx \right\} dt - \int_\Omega \lambda^\nu\, \nabla\cdot\mathbf{w}\, dx\,, \tag{6}$$

where $\lambda^\nu \in L^2(\Omega)\times(0,T)$ denotes the Lagrange multiplier. A standard variational procedure grants the saddle point system for the Lagrange (6): Find $(\mathbf{b}^\nu,\lambda^\nu) \in \mathcal{B}\times(0,T)\times L^2(\Omega)\times(0,T)$ satisfying

$$\begin{aligned} a(\mathbf{b}^\nu,\mathbf{w}) + c(\mathbf{w},\lambda^\nu) &= \langle f,\mathbf{w}\rangle \qquad \forall\, \mathbf{w}\in\mathcal{B} \quad t\in(0,T)\,,\\ c(\mathbf{b}^\nu,\mu) &= 0 \qquad \forall\, \mu\in L^2(\Omega), \quad t\in(0,T)\,, \end{aligned} \tag{7}$$

where the bilinear forms are defined as

$$a(\mathbf{b}^\nu, \mathbf{w}) \coloneqq \int_0^T \left\{ \int_\Omega \mathbf{w} \cdot \big(\nabla\phi \otimes \nabla\phi\big)\mathbf{b}^\nu \, dx + \nu^2 \int_\Omega \mathbf{w} \cdot \mathbf{b} \, dx \right\} dt$$

$$c(\mathbf{b}^\nu, \mu) \coloneqq \int_0^T \int_\Omega \mu(\nabla \cdot \mathbf{b}^\nu) \, dx \, dt \,,$$

and duality pairing

$$\langle f, \mathbf{w} \rangle \coloneqq - \int_0^T \int_\Omega \phi_t \, (\mathbf{w} \cdot \nabla\phi) \, dx \, dt \,.$$

If we suppose that ϕ is a classical solution to the advection equation (1) with $\mathbf{b}^\nu$ possessing a classical divergence, then the variational formulation (7) has the classical formulation

$$(8) \qquad \begin{cases} \big(\nabla\phi \otimes \nabla\phi + \nu \mathbf{I}\big)\mathbf{b}^\nu - \nabla\lambda^\nu = -\phi_t \, \nabla\phi & \text{over } \Omega \times (0,T)\,, \\ \nabla \cdot \mathbf{b}^\nu = 0 & \text{over } \Omega \times (0,T)\,, \\ \mathbf{b}^\nu \cdot \mathbf{n} = 0 & \text{on } \Gamma \times (0,T)\,, \\ \phi = 0 & \text{on } \partial\Omega \setminus \Gamma \times (0,T)\,. \end{cases}$$

The saddle point system (7) is well-posed when the bilinear forms $a(\cdot,\cdot)$ and $c(\cdot,\cdot)$ are V-elliptic and satisfy the inf-sup conditions, respectively; see, for instance, the textbook discussion [4, Chap.III, §4]. That the latter condition holds is a consequence of the choice of product space $\mathcal{B} \times L^2(\Omega)$ arising for the mixed formulation of the Poisson equation augmented with a homogeneous Dirichlet boundary condition on $\partial\Omega/\Gamma$; see [4, Chap.III, §4] for details. The condition that $a_\nu(\cdot,\cdot)$ is V-elliptic holds because

$$(9) \quad \begin{aligned} a(\mathbf{w}, \mathbf{w}) &= a(\mathbf{w}, \mathbf{w}) + \nu^2 \int_0^T \int_\Omega (\nabla \cdot \mathbf{w})^2 \, dx \, dt \\ &\geq \nu^2 \int_0^T \int_\Omega \big(\mathbf{w} \cdot \mathbf{w} + (\nabla \cdot \mathbf{w})^2\big) \, dx \, dt \; = \nu^2 T \|\mathbf{w}\|_{\mathcal{B}}^2 \qquad \forall\, \mathbf{w} \in \mathcal{B}\,, \end{aligned}$$

where the first equality holds since $\nabla \cdot \mathbf{w} = 0$. The resulting saddle point system now satisfies both conditions and so is well-posed. We remark that the regularization parameter ν must be positive. Otherwise the bilinear form $a_{\nu=0}(\cdot,\cdot)$ cannot be V-elliptic because

$$a_{\nu=0}(\mathbf{w}, \mathbf{w}) = \int_0^T \int_\Omega \big(\mathbf{w} \cdot \nabla\phi\big)^2 \, dx \, dt$$

cannot be identified with $\|\mathbf{w}\|_{\mathcal{B}}$ since $\nabla\phi$ is an element of $[L_2(\Omega)]^2$ containing $\mathcal{B}$ as a proper subspace. This demonstrates that the saddle point system (7) is ill-posed when not regularized so that consequently the minimization problem (3) is ill-posed.

This somewhat abstract explanation also has an elementary interpretation that also serves to underscore the roles of constraining and regularizing. Recall that $\bar{\mathbf{b}}$, given by (2c), can be added to any solution of the normal equations (2b). By imposing the constraint that any of these solutions are solenoidal, one function is identified (and given by the least squares problem (3)) but unfortunately does not depend continuously upon the data $\phi_t \, \nabla\phi$. This is because, in contrast to an algebraic saddle point linear system, the coefficient matrix $\nabla\phi \otimes \nabla\phi$ cannot simply be invertible on the nullspace of the divergence operator $\nabla\cdot$. The more stringent condition of V-ellipticity is required and cannot be satisfied since the function $\psi : \Omega \to \mathbb{R}$ in $\bar{\mathbf{b}}$ can always be chosen so that the ratio

$$\frac{a_{\nu=0}(\mathbf{w},\mathbf{w})}{\|\mathbf{w}\|_{\mathcal{B}}}$$

has no positive lower bound for all $\mathbf{w} \in \mathcal{B}$ and so the least squares problem (3) is ill-posed. Hence the specified regularization provides the needed ellipticity and the velocity can be stably estimated.

3. A Mixed Finite Element Method.

A mixed finite element method for the saddle point system (7) results when finite dimensional subspaces $\mathcal{B}_h$ and $L^2_h(\Omega)$ are selected leading to the discrete saddle point problem: Find $(\mathbf{b}^\nu_h, \lambda^\nu_h) \in \mathcal{B}_h \times (0,T) \times L^2_h(\Omega) \times (0,T)$ satisfying

$$\begin{aligned} a(\mathbf{b}^\nu_h,\mathbf{w}) + c(\mathbf{w},\lambda^\nu_h) &= \langle f,\mathbf{w}\rangle \qquad \forall\, \mathbf{w} \in \mathcal{B}_h \quad t \in (0,T)\,,\\ c(\mathbf{b}^\nu_h,\mu) &= 0 \qquad\quad \forall\, \mu \in L^2_h(\Omega) \quad t \in (0,T)\,. \end{aligned} \tag{10}$$

In contrast to a standard finite element formulation, the discrete formulation is not automatically well-posed even when $\mathcal{B}_h \subset \mathcal{B}$ and $L^2_h(\Omega) \subset L^2(\Omega)$. The parameterized family of subspaces $\mathcal{B}_h, L^2_h(\Omega)$ must satisfy the Babuška–Brezzi conditions, see, for instance the textbook discussion in [4, Chap.III, §4]. These conditions are the discrete analogues of the V-elliptic and inf-sup conditions needed to show that the infinite dimensional problem is well-posed. Satisfying the Babuška–Brezzi conditions for a specific pair of finite element basis functions is often a challenge. Fortunately, there are several choices of element pairings $(\mathbf{b}^\nu_h, \lambda^\nu_h)$ for the mixed finite element formulation of the Poisson equation augmented with a homogeneous Dirichlet boundary condition on $\partial\Omega/\Gamma$.

The pairing we employ is the Raviart–Thomas elements introduced in [10] for discrete approximation in $H_{\mathrm{div}}(\Omega)$; see, e.g., [4, Chap.III, §4] for a discussion. Let $\mathcal{T}_h$ be a triangulation on Ω with K representing a particular triangle. The finite dimensional subspaces associated with the lowest order Raviart–Thomas elements on triangles are defined as follows:

(11a)
$$\mathcal{B}_h \coloneqq \{\big(b^{(1)}_K(t), b^{(2)}_K(t)\big) \in \mathcal{B} \mid (a^{(1)}_K(t), a^{(2)}_K(t)) + d_K(t)(x,y)\,; a^{(i)}_K(t), d_K(t), \in \mathbb{R}; K \in \mathcal{T}_h\}$$
(11b)
$$L^2_h(\Omega) \coloneqq \{\lambda^\nu_K(t) \mid \lambda^\nu(t) = \text{a constant on each triangle } K \in \mathcal{T}_h\}\,.$$

This leads to the finite element interpolant functions

$$\mathbf{b}^\nu_h(x,y,t) = \sum_{K\in\mathcal{T}} \big(b^{(1)}_K(t), b^{(2)}_K(t)\big)\mathbb{1}_K(x,y)\,, \tag{11c}$$

$$\lambda^\nu_h(x,y,t) = \sum_{K\in\mathcal{T}} \lambda^\nu_K(t)\mathbb{1}_K(x,y)\,. \tag{11d}$$

Inserting the interpolants into (10) and testing against each of the basis functions leads to the semi-discrete saddle point system

$$\begin{bmatrix}\mathbf{A} & \mathbf{C}^T\\ \mathbf{C} & \mathbf{0}\end{bmatrix}\begin{bmatrix}\mathbf{p}\\ \mathbf{q}\end{bmatrix} = \begin{bmatrix}\mathbf{f}\\ \mathbf{0}\end{bmatrix} \qquad t \in (0,T)\,. \tag{12}$$

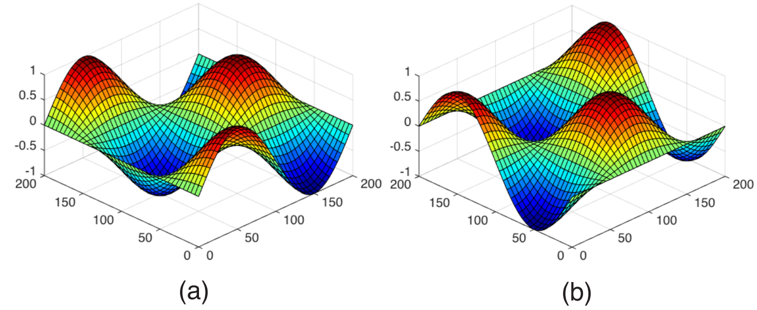

FIG. 1. *The components of the velocity* $\mathbf{c}$ *given by* (16b) *(a) x-component (b) y-component.*

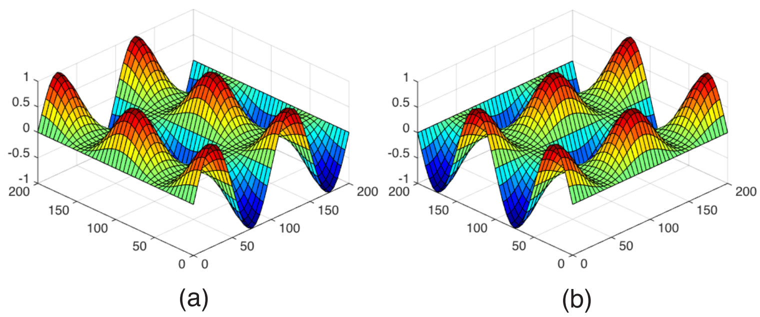

FIG. 2. *The components of the velocity* $\mathbf{d}$ *given by* (16c) *(a) x-component (b) y-component.*

Given some ordering of the elements, the entries of the matrices $\mathbf{A}$ and $\mathbf{B}$ are given by

$$a_\nu\big((b_i^{(1)}, b_i^{(2)}), (b_j^{(1)}, b_j^{(2)})\big)\,, \qquad i, j = 1, \cdots, 3N \tag{13a}$$

$$c\big((b_j^{(1)}, b_j^{(2)}), \lambda_k^\nu\big)\,, \qquad k = 1, \cdots, N \tag{13b}$$

respectively. The vectors $\mathbf{p} \in \mathbf{R}^{3N}$ and $\mathbf{q} \in \mathbf{R}^N$ contain the coefficients for the basis functions and the vector $\mathbf{f}$ has entries

$$\langle f, (b_i^{(1)}, b_i^{(2)})\rangle\,, \qquad i = 1, \cdots, 3N\,. \tag{13c}$$

4. Example. Our example verifies that the mixed finite element method we propose for the discretization of the regularized saddle point system (7) correctly approximates the solenoidal component of the solution of the inverse problem given by the constrained minimization (3). We first derive a closed form solution to the inverse problem for the classical formulation of (7) when $\nu = 0$, i.e., the optimality system for (3). Recall that we have established that this latter least squares problem is ill-posed (see end of §2) and so will enable us to quantify the influence of the regularization parameter ν.

Let $\Omega = (0, L) \times (0, L) = (0, L)^2$ and $\Gamma = \partial(0, L)^2$ so that $\partial\Omega \setminus \Gamma = \emptyset$. Given an intensity ϕ satisfying a pure Neumann boundary condition on Γ, we derive a closed

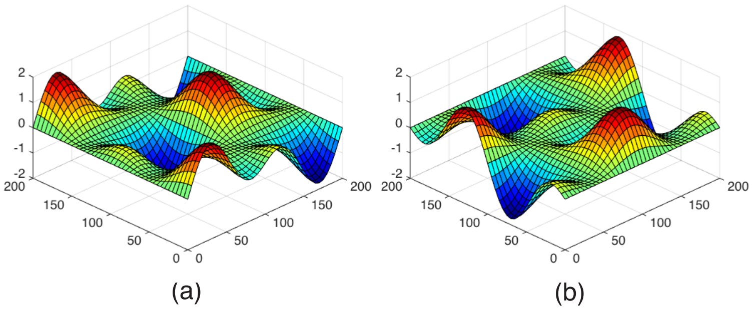

FIG. 3. *The components of the velocity* $\mathbf{c}+\mathbf{d}$ *given by* (16b)–(16c) *(a) x-component (b) y-component.*

form expression for the velocity $\mathbf{b}$ satisfying

$$\left\{\begin{aligned} \big(\nabla\phi\otimes\nabla\phi\big)\mathbf{b}-\nabla\lambda &= -\phi_t\,\nabla\phi && \text{over } \Omega\times(0,T)\,,\\ \nabla\cdot\mathbf{b} &= 0 && \text{over } \Omega\times(0,T)\,,\\ \mathbf{b}\cdot\mathbf{n} &= 0 && \text{on } \Gamma\times(0,T)\,. \end{aligned}\right. \tag{14}$$

Because the function $\phi(x,y,t)=\phi\big(x-v_1(x,y)\,t,y-v_2(x,y)\big)$ solves (1) given the spatially varying velocity $\mathbf{v}(x,y)=\big(v_1(x,y),v_2(x,y)\big)$, then $\phi_t=-\mathbf{v}\cdot\nabla\phi_0$ so that a collection of solenoidal velocities is given by

$$\mathbf{b}=(1+\sigma)\mathbf{c} \text{ with } \sigma=\frac{\nabla\cdot[(\nabla\phi\cdot\mathbf{d})J\,\nabla\phi]}{\nabla\cdot[(\nabla\phi\cdot\mathbf{c})J\,\nabla\phi]}\,, \tag{15a}$$

where $(\nabla\phi\cdot\mathbf{c})J\,\nabla\phi$ is not irrotational, J is given in (2c)

$$\mathbf{v}=\mathbf{c}+\mathbf{d}\,,\ \text{satisfies } \nabla\cdot\mathbf{c}=0\,,\nabla\times\mathbf{d}=\mathbf{0}\,, \tag{15b}$$

and $\mathbf{c}$ satisfies the velocity boundary condition.[1] That a multitude of velocities satisfy (14) is a direct manifestation that the optimization problem (3) is ill-posed, as explained following equation (9). The requisite Lagrange multiplier λ is then given by the solution of the pure Neumann boundary value problem

$$\left\{\begin{aligned} &\Delta\lambda=\nabla\cdot\big((\nabla\phi\cdot(\sigma\mathbf{c}-\mathbf{d}))\nabla\phi_0\big) && \text{over } \Omega\,,\\ &\nabla\lambda\cdot\mathbf{n}=0\,, && \text{on } \Gamma\,, \end{aligned}\right. \tag{15c}$$

The solution of the above Neumann boundary value problem is unique up to a constant since the data is of zero mean, i.e.,

$$\int_\Omega \nabla\cdot\big((\nabla\phi\cdot(\sigma\mathbf{c}-\mathbf{d}))\nabla\phi_0\big)\,dx=\int_{\partial\Omega}\big(\nabla\phi\cdot(\sigma\mathbf{c}-\mathbf{d})\big)\nabla\phi_0\cdot\mathbf{n}\,dx=0\,,$$

given the pure Neumann boundary conditions for the advection equation (1). That the solution of (15c) is only unique up to a constant is irrelevant because only the gradient of the Lagrange multiplier is needed for the saddle point system (14).

[1]Such a representation of $\mathbf{v}$ is given by the Helmholtz-Hodge decomposition; see [5] and the well-written survey [3]. We also exploited the identity that $\nabla\times\mathbf{z}=-\nabla\cdot(J\mathbf{z})$ for a vector with two components.

The velocity solution (15a) exemplifies that only a solenoidal component of $\mathbf{v}$ can be recovered and the gradient of the Lagrange multiplier corrects for the irrotational component of $\mathbf{v}$. Moreover, this solution is only defined when $\mathbf{c}$ is not orthogonal to $\nabla\phi$—this is a consequence of the aperture problem reviewed following the least squares problem (2b) that while including a constraint renders a solution to the (constrained) least squares problem unique, the estimated velocity can only recover an isochoric component of the motion. Otherwise when $\nabla\phi \cdot \mathbf{c} = 0$ then $\mathbf{b} = \mathbf{0}$; in particular, if the solenoidal component is null so is $\mathbf{b}$.

Several additional cases are of interest. First, if $\nabla\phi \cdot \mathbf{d} = 0$ then $\sigma = 0$ and $\mathbf{b} = \mathbf{c}$; in other words, the underlying velocity $\mathbf{v}$ can be recovered if the irrotational component of the motion is orthogonal to $\nabla\phi$. In particular, if the motion is solenoidal, then the motion can be reconstructed. Second, if the solenoidal and irrotational components of $\mathbf{v}$ in the direction of $\nabla\phi$ are equal, then the velocity $\mathbf{b} = 2\mathbf{c}$ and the Lagrange multiplier is a constant. Third, if the solenoidal and irrotational components of $\mathbf{v}$ in the direction of $\nabla\phi$ are equal and opposite, then the velocity $\mathbf{b} = \mathbf{0}$ and $\nabla\lambda = -2(\nabla\phi \cdot \mathbf{d})\nabla\phi$.

We can also contrast the solution of (8) with the solution of (14). If we express the solution $\mathbf{b}^\nu = \mathbf{b} + \mathbf{e}$ and $\lambda^\nu = \lambda + \mu$, insert into (8) and invoke (14), then the corrections $(\mathbf{e}, \mu)$ satisfy the saddle point system

$$\begin{cases} \big(\nabla\phi \otimes \nabla\phi + \nu\mathbf{I}\big)\mathbf{e} - \nabla\mu = -\nu(1+\sigma)\mathbf{c} & \text{over } \Omega \times (0,T)\,, \\ \nabla \cdot \mathbf{e} = 0 & \text{over } \Omega \times (0,T)\,, \\ \mathbf{e} \cdot \mathbf{n} = 0 & \text{on } \Gamma \times (0,T)\,. \end{cases}$$

In words, the corrections solve a steady-state problem with velocity data given by the solution (15a). If the regularization parameter ν is set to zero, then $(\mathbf{e} = \mathbf{0}, \mu = 0)$ explaining that there is no correction to the unregularized problem; this also the case if $\sigma = -1$, a situation considered in the previous paragraph.

To verify our numerical solution, we select the initial intensity

$$\phi_0(x,y) = -\xi^{-1}\big(\cos\xi x \cos\xi(x-L) + \cos\xi y \cos\xi(y-L)\big)\,, \qquad \xi = \frac{n\pi}{L}\,,$$

so that

$$\phi(x,y,t) = \phi_0\big(x - v_1(x,y)t, y - v_2(x,y)t\big) \tag{16a}$$

solves the advection equation (1) with pure Neumann boundary conditions. We consider the velocity field $\mathbf{v} = \mathbf{c} + \tau\,\mathbf{d}$ for a real number τ where

$$\mathbf{c}\big(x,y\big) = \big(\sin\gamma x \cos\gamma y, -\cos\gamma x \sin\gamma y\big)\,, \quad \gamma = \frac{m\pi}{L}\,, \tag{16b}$$

$$\mathbf{d}(x,y) = -\delta^{-1}\nabla\big(\cos\delta x \cos\delta(x-L) \cos\delta y \cos\delta(y-L)\big)\,, \qquad \delta = \frac{i\pi}{L}\,. \tag{16c}$$

Both vector fields satisfy the velocity boundary condition when the former and latter vector fields are solenoidal and irrotational, respectively. Figures 1–3 display the velocities $\mathbf{c}$, $\mathbf{d}$ and $\mathbf{c} + \mathbf{d}$ when $n = 10.0$, $m = 2.0$, and $i = 2.0$.

Figure 4 shows the order h velocity approximation $\mathbf{b}_h^\nu$ when $\mathbf{v}$ is solenoidal (or $\tau = 0$) that solves the discrete saddle point system (10) given the mixed finite element method presented in section 3 with a mesh size of 4 units and regularization parameter $\nu = 1$. Figure 5 displays the inverse mesh size h against the error $\|\mathbf{b}_h - \mathbf{c}\|_{[L^2\Omega]^2}$ for

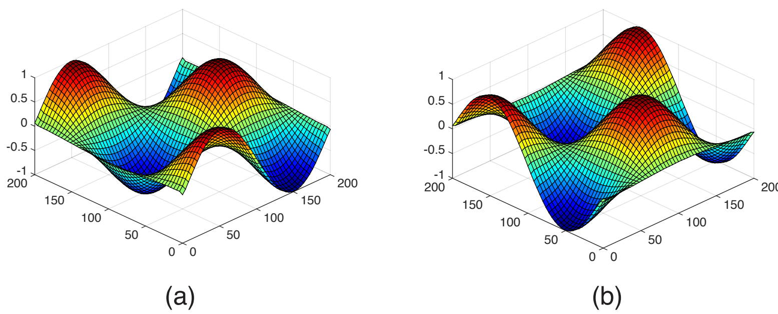

FIG. 4. *Velocity approximation* $\mathbf{b}_h^\nu$ *given the mixed finite element method presented in section 3 with a mesh size of 4 units (a) x-component (b) y-component*

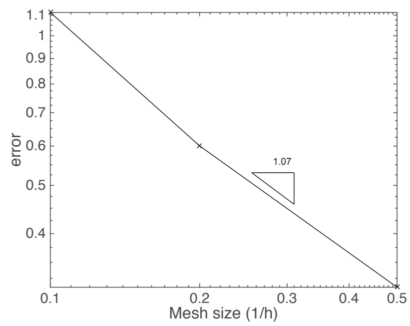

FIG. 5. *Convergence of the mixed finite element formulation for the velocity field,* b_x^ν. *The velocity error in x and y are similar.*

three choices of mesh size h. The slope of the line connecting the three points is the rate of convergence that confirms the predicted rate for the RT0 element. Our experiments were implemented in MATLAB and the saddle point linear systems were solved using MATLAB's sparse direct solver.

In Figure 6 we show the influence of the regularization parameter ν for large and small values. The results suggest a minimum value, approximately 1, below which oscillations emerge in the solution. The velocity results for $\nu = 0$ (or no regularization) are shown in Figure 7. Figure 8 demonstrates that the solenoidal component (16b) of the solution is accurately computed for a range of frequencies. We show the computed x-velocity component as m is increased from 2 to 16. The error for each m is also shown in this figure. Although the discretization error increases with m as expected, the estimated velocity does not exhibit spurious oscillations as in Figure 7.

The results of our numerical experiment confirm that our proposed constrained regularized least squares functional and ensuing finite element method indeed approximate the sought after solenoidal velocity field.

5. Conclusions.

Our paper presented a novel constrained, regularized least squares problem and ensuing mixed finite element method to estimate the velocity for the optical flow constraint. This is in contrast to other regularization techniques for which the solution is composed of an unknown combination of divergence and curl-free components. The crucial distinction is that we have incorporated a constraint into the formulation of the problem. While, our specific choice of linear constraint assumes

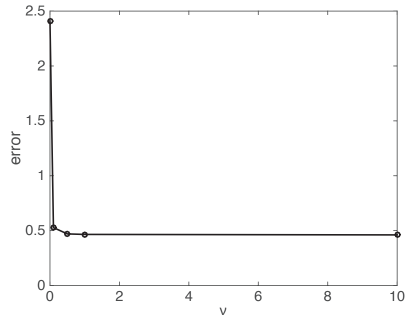

FIG. 6. *Solution error (for the x-component of the velocity) vs. the regularization parameter ν. The results in x and y are again similar*

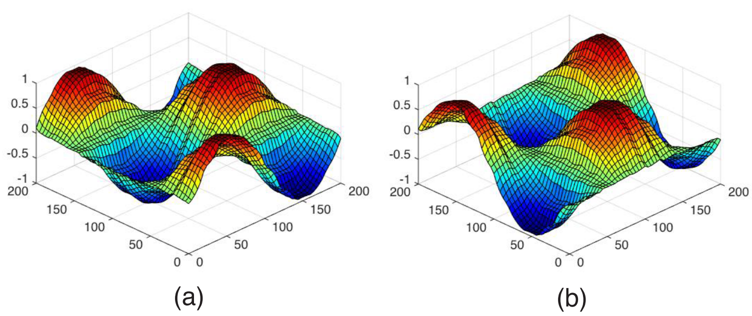

FIG. 7. *Velocity approximation $\mathbf{b}_h^\nu$ for $\nu = 0$ (no regularization) and a mesh size of 4 units; (a) x-component (b) y-component. The effect of no regularization is apparent; because the saddle point system (14) is ill-posed the numerical solution exhibits oscillations.*

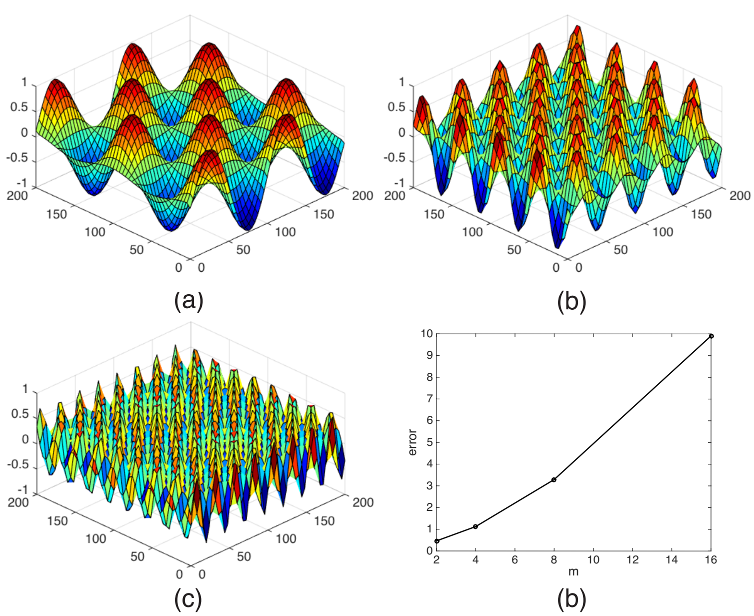

FIG. 8. *Velocity approximation $\mathbf{b}_h^\nu$ for varying m for a mesh size of 4 units (only the x-component is shown). (a) $m = 4.0$ (b) $m = 8.0$ (c) $m = 16.0$ (d) solution error vs. m*

that the velocity is solenoidal, other choices are possible, e.g., specifying some rotational component of the velocity, for instance that the velocity is irrotational. The numerical example confirmed our analyses and also introduced a closed form solution for the unregularized constrained least squares problem (3). This enables us to assess the velocity approximation estimated to be compared to the exact solution.

Acknowledgments. We thank Dr. Drew Kouri of Sandia National Labs for several helpful discussions, including bringing to our attention the paper [8]. We also thank Dr. Phillip Reu for his many helpful discussions on the DIC problem.

REFERENCES

[1] G. Aubert and P. Kornprobst, *Mathematical Problems in Image Processing*, vol. 147 of Applied Mathematical Sciences, Springer-Verlag New York, 2 ed., 2006.

[2] M. Bertero, T. A. Pogcio, and V. Torre, *Ill-posed problems in early vision*, in Proceedings of the IEEE, 1988, pp. 869–889, doi:10.1109/5.5962.

[3] H. Bhatia, G. Norgard, V. Pascucci, and P. T. Bremer, *The Helmholtz-Hodge decomposition—a survey*, IEEE Transactions on Visualization and Computer Graphics, 19 (2013), pp. 1386–1404, doi:10.1109/TVCG.2012.316.

[4] D. Braess, *Finite Elements*, Cambridge University Press, third ed., 2007, http://dx.doi.org/10.1017/CBO9780511618635. Cambridge Books Online.

[5] A. J. Chorin and J. E. Marsden, *A Mathematical Introduction to Fluid Mechanics*, no. 4 in Texts in Applied Mathematics, Springer-Verlag New York, 3 ed., 1993, doi:10.1007/978-1-4612-0883-9.

[6] M. Fortin and R. Glowinski, *Augmented Lagrangian Methods: Applications to the Numerical Solution of Boundary-Value Problems*, Studies in Mathematics and its Applications, Elsevier Science, 2000, https://books.google.com/books?id=s6_5EeBjQnkC.

[7] B. K. Horn and B. G. Schunck, *Determining optical flow*, Artificial Intelligence, 17 (1981), pp. 185–203, doi:http://dx.doi.org/10.1016/0004-3702(81)90024-2, http://www.sciencedirect.com/science/article/pii/0004370281900242.

[8] K. Ito and K. Kunisch, *Estimation of the convection coefficient in elliptic equations*, Inverse Problems, 13 (1997), p. 995, http://stacks.iop.org/0266-5611/13/i=4/a=007.

[9] R. B. Lehoucq, D. Z. Turner, and C. A. Garavito-Garźon, *PDE constrained optimization for digital image correlation*, Technical Report SAND2015-8515, Sandia National Laboratories, 2015.

[10] P.-A. Raviart and J.-M. Thomas, *A mixed finite element method for 2-nd order elliptic problems*, in Mathematical aspects of finite element methods, Springer, 1977, pp. 292–315.

[11] C. Schnörr, *Determining optical flow for irregular domains by minimizing quadratic functionals of a certain class*, International Journal of Computer Vision, 6 (1991), pp. 25–38, doi:10.1007/BF00127124, http://dx.doi.org/10.1007/BF00127124.

[12] H. Schreier, J.-J. Orteu, and M. A. Sutton, *Image correlation for shape, motion and deformation measurements*, Springer US, 2009.

[13] J. Weickert and C. Schnörr, *A theoretical framework for convex regularizers in pde-based computation of image motion*, International Journal of Computer Vision, 45 (2001), pp. 245–264, doi:10.1023/A:1013614317973, http://dx.doi.org/10.1023/A:1013614317973.